# APPLICATION OF A PREDICTIVE MODEL FOR BRITTLE FRACTURE IN A HIGH STRENGTH STEEL AND ITS WELD

R. Rodríguez-Martín, I. Ocaña, A. Martín-Meizoso
CEIT, Centro de Estudios e Investigaciones Técnicas de Guipúzcoa and
TECNUN, Escuela Superior de Ingenieros, Universidad de Navarra
Paseo Manuel de Lardizábal, 15, 20018 San Sebastián, Spain
rarodriguez@ceit.es, iocana@ceit.es, ameizoso@ceit.es

## Abstract

High strength steels are characterized by their high value of yield strength but for many applications other properties like toughness, ductility, and weldability are also required. With the objective of comparing the toughness of a steel and its weld in the lower shelf, fracture tests were performed. A predictive model for brittle fracture has been validated using volume fraction and size distribution of brittle particles and phases for the two steels. The model is based on the "weakest-link" hypothesis and takes into account the presence of two independent distributions of structural elements (isolated particles and matrix grains) with two barriers for cleavage propagation (the particle/matrix interfaces and the grain boundaries), characterized by a crack arrest capability well over the crack propagation resistance of the cleavage of the crystalline lattice of the two phases.

## Introduction

Catastrophic fracture of materials can be understood if they are considered as a whole of independent structural unities resistant to failure. If only one of these unities breaks, the material fails by cleavage. On this assumption, well known as "weakest link" hypothesis, a predictive model for brittle fracture has been developed.

In a metallic matrix with a dispersion of non-metallic brittle particles or inclusions with a size smaller than the grain size of the metallic matrix, the nucleating event of a macroscopic failure results from three simple events: slip-induced cleavage of a particle, propagation of the microcrack to the neighbouring grains across the particle-matrix, and then transmission across the grain boundaries to neighbouring grains. The predictive model of brittle fracture takes into account these three steps and calculates failure probability, by using as input data, volume fraction and size distribution of brittle particles and present phases. In this paper, an application of the model for the prediction of fracture toughness of a high strength steel ($\sigma_Y$=690 MPa) and its weld is presented.

## Materials and experimental procedure

In Table 1 the chemical composition of the steels is shown. The base material P690Q was produced by means of a quenching and tempering treatment and the same procedure was followed for P690Q welded after performing the welding process.

TABLE 1. Chemical composition of steels (wt %).

| Material | C | Si | Mn | Cr | Mo | Ni | Al | Cu | V | B |
|---|---|---|---|---|---|---|---|---|---|---|
| P690Q | 0.14 | 0.31 | 0.83 | 0.61 | 0.42 | 1.01 | 0.04 | 0.27 | 0.05 | 0.003 |
| P690Q_W | 0.06 | 0.31 | 1.40 | 0.50 | 0.36 | 2.21 | 0.02 | 0.11 | 0.02 | <0.0005 |

Tensile tests at low temperatures were performed in order to determine the elastic limit and the hardening exponent of the steels. Specimen geometry is specified in Fig. 1. Tests were carried out following ASTM E8M-89 standard [1].

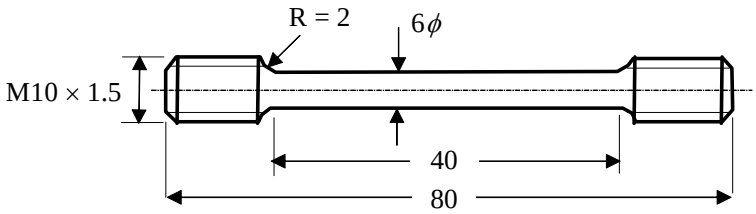


FIGURE 1. Tensile test specimen geometry.

Compact tensile specimens were machined and precracked to analyze the fracture toughness for the two steels. In the particular case of the welded specimens, the most brittle zone in the HAZ is expected to be the CGHAZ adjacent to the weld bed, therefore the notch was machined by cutting the maximum amount of this microstructure (Fig. 2). Fracture tests were performed at very low temperatures to assure a brittle behaviour and in accordance with ESIS P2-91D standard [2]. After breaking the specimens, fractographic analyses were carried out to determine the fracture mechanisms and the initiation sites for the brittle fracture.

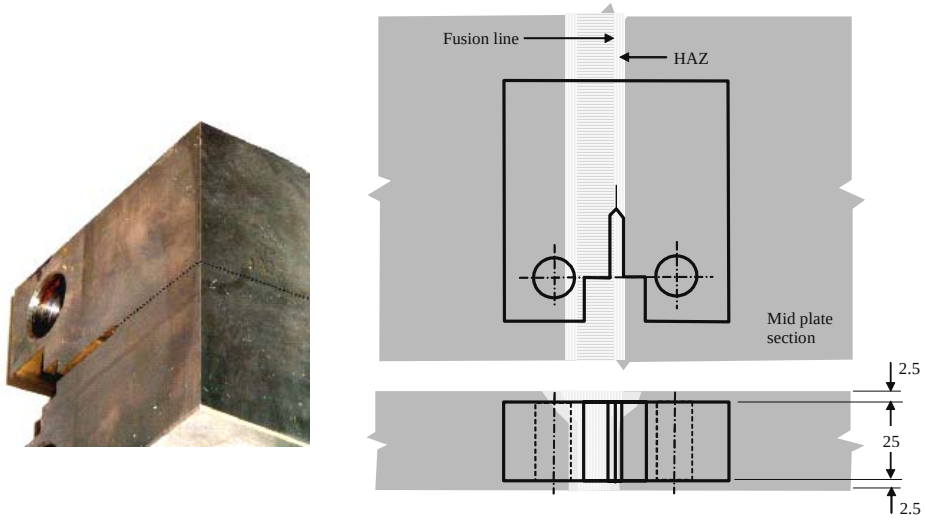


FIGURE 2. Scheme of the procedure of extraction of test pieces in the welded material.

An exhaustive microstructural characterization was carried out for the two steels. Specimens were polished and etched using Nital. A quantification of the microstructures was also performed in order to enter the data into the predictive fracture model.

## Results and discussion

### *Microstructural characterization*

As it is well known, fracture toughness depends to a great extent on the microstructure. In order to determine the microstructure over the fracture path, metallographic specimens were polished and etched along the fracture plane. P690Q steel showed a strongly tempered martensitic microstructure (Fig.3). In the case of the welded material, the microstructural heterogeneity in the HAZ near the weld beds affects the mechanical properties. In order to achieve a better understanding of the mechanical behaviour of the different microstructures in the HAZ by the deposited weld beds, some micro-hardness tests combined with metallography were performed (Fig.4). The most brittle microstructure is expected to be near the weld bed, with a very high hardness and a quite coarse grain size.

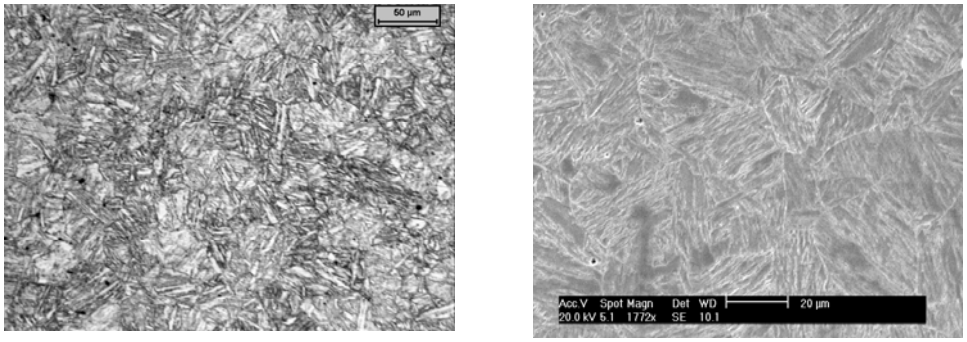


a) b)

FIGURE 3. Microstructure of P690Q, a) optical micrograph, b) scanning electron micrograph.

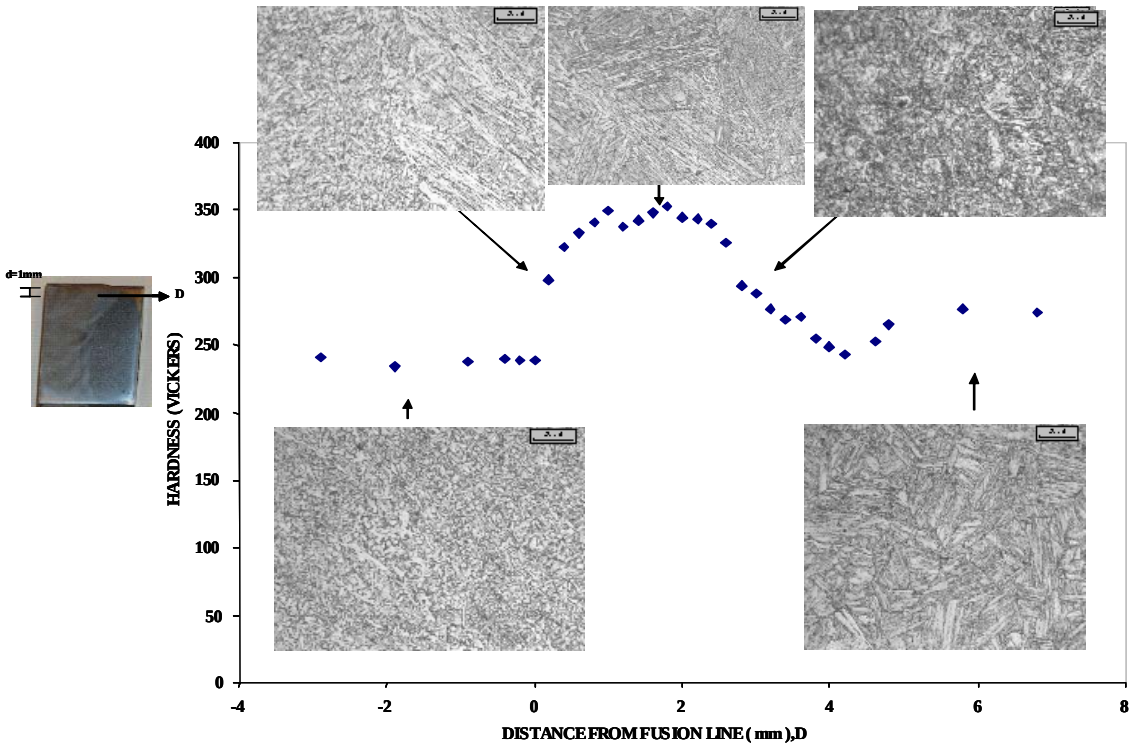


FIGURE 4. Micro-hardness profile at 1 mm from the top of the specimen. The most relevant microstructural zones are detailed.

Quantitative measurements of volume fraction and size distribution were performed for martensite and inclusions present in P690Q. Fractography of broken specimens of the welded material showed that the martensite present in the HAZ was the phase responsible for the brittle fracture, therefore, quantitative measurements were carried out for this phase and also for inclusions as initiation triggers. Size distributions were fitted to a four-parameter gamma function (Eq. 1), as required by the predictive model.

$$f(x) = \frac{c \cdot a^{p}}{\Gamma(p)} \cdot (x-d)^{cp-1} \cdot e^{-a(x-d)^{c}} \tag{1}$$

The parameters *a*, *p*, *c* and *d*, were produced by means of a least square fitting. Table 2 shows the results.

TABLE 2. Volume fraction and fitting parameters for all microstructural characteristics of the two steels.

| | | *f* | *c* | *a* | *p* | *d* |
|---|---|---|---|---|---|---|
| P690Q | Martensite | 1 | 0.3 | 16.46 | 37.38 | 0 |
| | Inclusions | $2x10^{-3}$ | 0.3 | 66.61 | 60.42 | 0 |
| P690Q_W | Martensite | 1 | 0.3 | 18.35 | 39.86 | 0 |
| | Inclusions | $1.8x10^{-3}$ | 0.3 | 72.31 | 62.04 | 0 |

In all cases the best fitting was obtained with d=0 (three-parameter gamma function). The 3-parameter gamma fittings for martensitic packets and for inclusions in P690Q are illustrated in Fig. 5.

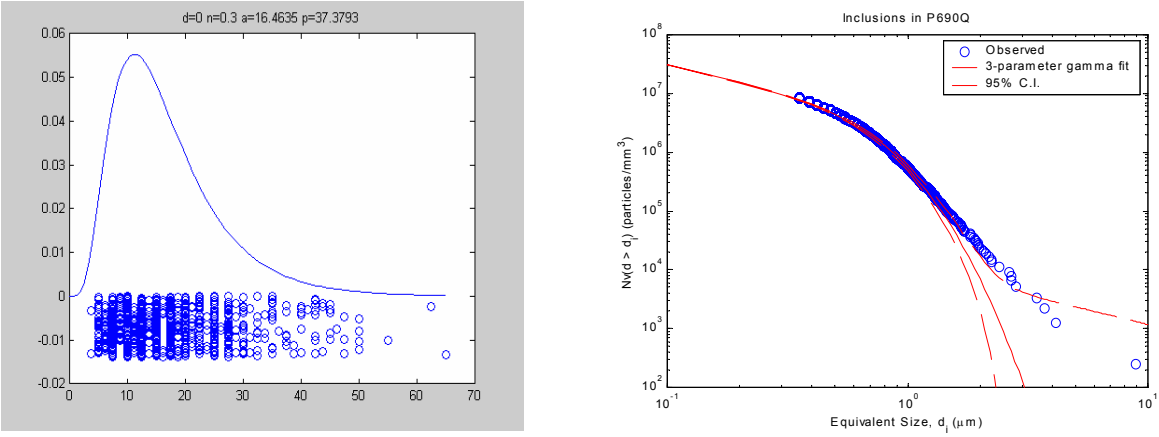


a) b)

FIGURE 5. a) 3-parameter gamma function for martensitic packets in P690Q, b) size distribution for inclusions in P690Q.

***Tensile tests***

The predictive model for brittle fracture takes into account the plastic behaviour of the material because of the presence of plastic deformation in the crack tip. This fact is accounted for by fitting tensile test data to Hollomon's (Eq. 2).

$$\sigma = \sigma_0 \cdot \left( \frac{\varepsilon}{\varepsilon_0} \right)^n \tag{2}$$

As for P690Q welded material, it was impossible to machine tensile specimens in the exact zone where CT(TL) specimens were precracked. $\sigma_0$ was calculated taking into account the relation between micro-hardness values of the welded material and the base material. This relation turned out to be approximately 1.3, and was higher for the welded material (Eq. 3).

$$\sigma_{0HAZ} = \frac{HV_{HAZ}}{HV_{BaseMaterial}} \cdot \sigma_{0BaseMaterial} = 1.3 \cdot \sigma_{0BaseMaterial} \tag{3}$$

Figure 6 shows Hollomon's fitting for P690Q welded material at 77K, 156K and 179K, as calculated from Hollomon's fitting for the base material. All values for $\sigma$ are higher by a factor of 1.3 compared to those of the base material. The value of $n$, the hardening exponent, is considered the same as for the base material.

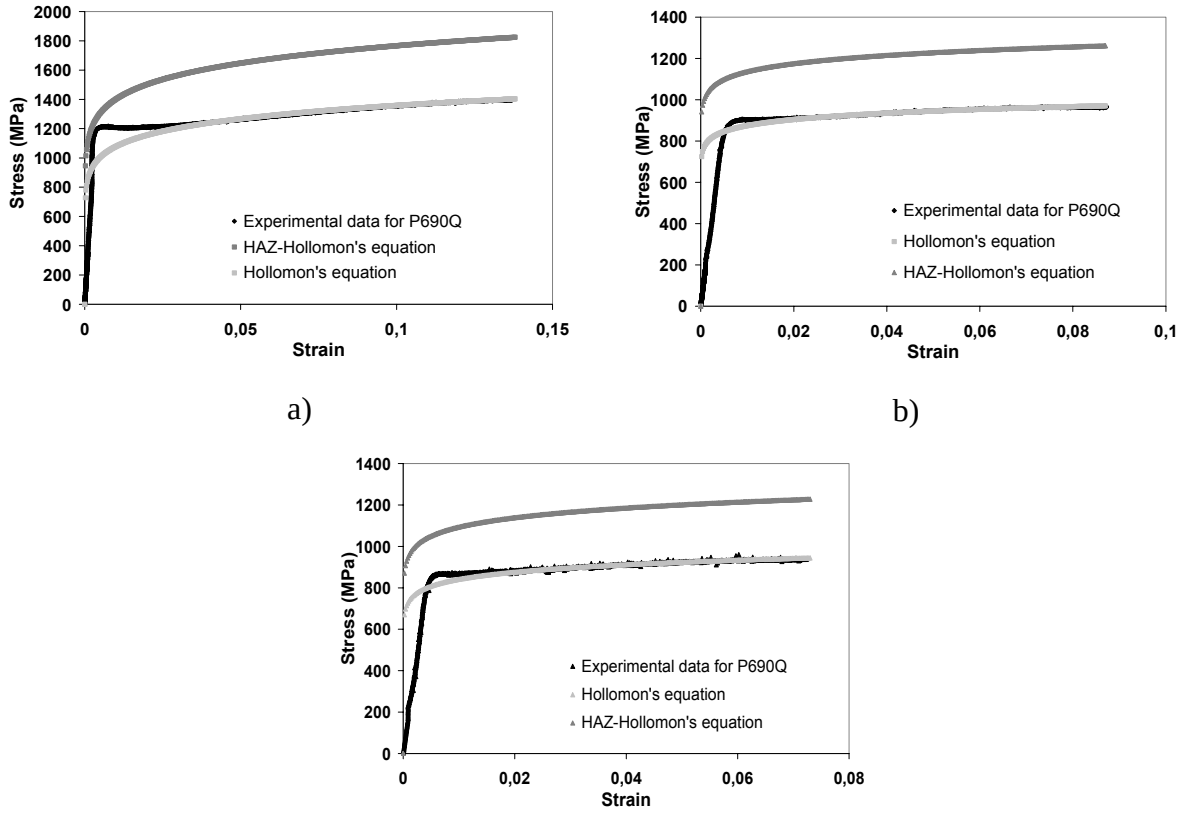


FIGURE 6. Hollomon's fitting for P690Q welded, a) 77K, b) 156K, c) 179K.

The results are summarized in Table 3. These values for $\sigma_0$ and $n$ were used as input data for the modelling of fracture behaviour of two steels.

TABLE 3. Yield strength and hardening exponent for P690Q_welded.

| | $T$ | $\sigma_0$ (MPa) | $n$ |
|---|---|---|---|
| P690Q | 77K | 916.8 | 0.1 |
| | 156K | 809 | 0.05 |
| | 179K | 766.3 | 0.06 |
| P690Q_welded | 77K | 1191.9 | 0.1 |
| | 156K | 1051.8 | 0.05 |
| | 179K | 996.2 | 0.06 |

***Fracture mechanics tests***

Compact tensile specimens of the two steels were fractured at 77K, 156K, and 179K to insure a brittle behaviour. Specimens showed a linear behaviour until fracture and fracture toughness was evaluated from Eq. 4 [2].

$$K_c = \frac{F_c}{B\sqrt{W}} f(a_0/W) \tag{4}$$

The usual trend for fracture toughness, increasing with temperature, was observed. Table 4 summarizes the results obtained for the two steels and conditions with the mean values and the standard deviation for all the measured values.

TABLE 4. Results for the fracture tests performed at low temperatures ($K_{Ic}$ in MPa√m).

| | P690Q | P690Q_welded |
|---|---|---|
| 77K | 42±6 | 53±4 |
| 156K | 154±36 | 105±25 |
| 179K | 176±27 | 149±26 |

***Modelling***

The predictive model estimates the probability of brittle fracture from the following microstructural parameters: grain size distribution, as well as, volume fraction and size distribution of brittle particles. The probability of microcrack nucleation in brittle particles, $\alpha$, and the crack arrest factors at different barriers (matrix/matrix, $K_{IC}^{m/m}$, and particle/matrix, $K_{IC}^{i/m}$), are fundamental parameters of the model, Martín-Meizoso *et al*. [3-5].

Experimental results for fracture toughness of the two high strength steels (the base material and its welds) were used to validate the model with the objective of confirming the dependence of the

probability of microcrack nucleation, $\alpha$, with temperature. The values for $K_{IC}^{m/m}$ and $K_{IC}^{i/m}$ agree with bibliography, Hahn [6]. Figure 7 shows model predictions together with experimental results for the two steels.

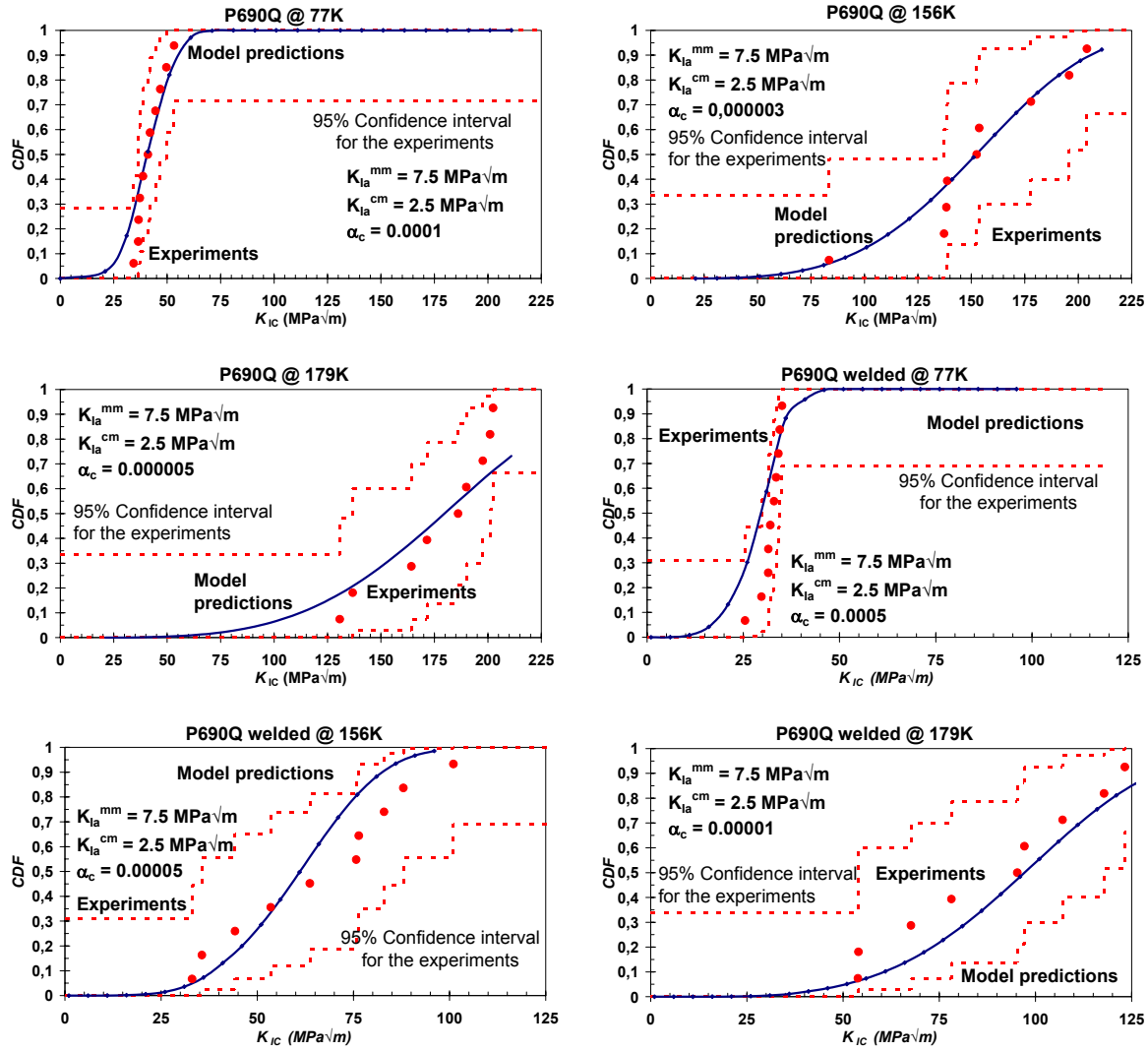


FIGURE 7. Model predictions and experimental results at 77K, 156K and 179K for P690Q steel and its weld.

## Conclusions

At the lowest temperatures, the toughness is controlled by the microcrack nucleation in brittle particles or second phases instead of by propagation across the matrix; a change in the values for $K_{IC}^{m/m}$ and $K_{IC}^{i/m}$ does not affect model predictions. The probability of brittle fracture of a microstructurally heterogeneous specimen (typical in HAZ), can also be predicted by the model. In order to simplify the modelling process, it is advised to have previously studied samples to determine the most dangerous microstructural zone in the HAZ. The model proposes a dependence for the probability of microcrack nucleation on temperature, and in this way, corrects the general tendency of previous models to underestimate the toughness.

## Acknowledgements

The financial support of this work by the Spanish C.I.C.Y.T. (MAT 2001-4275-E) and by C.E.C.A. (7210-PR-312) is gratefully acknowledged.

## References

1. Standard test methods for tension testing on metallic materials (metric) ASTM E8M-89.

2. ESIS procedure for determining the fracture behaviour of materials. ESIS P2-91D.

3. Martín-Meizoso, A., Ocaña-Arizcorreta, I., Gil-Sevillano, J. and Fuentes-Pérez, M., *Acta Metall*., vol. 42, 2057-2068, 1994.

4. Ocaña-Arizcorreta, I., Martín-Meizoso, A., Gil-Sevillano, J. and Fuentes-Pérez, M., *Anales de Mecánica de la Fractura*, vol. 10, 281-285, 1993.

5. Gil-Sevillano, J., Martín-Meizoso, A., and Fuentes-Pérez, M., *Anales de la Mecánica de Fractura*, vol. 8, 3-8, 1991.

6. Hahn, G.T. *Metall. Trans. A*, vol. 15A, 947, 1984.